Integrated Guidance and Control of a Missile in the Presence of Randomness in Disturbances*

Almıla Bektaş, Halit Ergezer

***Abstract*— In this paper, the effectiveness of an Integrated Guidance and Control (IGC) scheme of a skid-to-turn missile based on Global Terminal Sliding Mode Control (SMC) and reduced order Extended State Observer (ESO) is assessed in the presence of non-sinusoidal disturbances. Several studies in literature define the disturbances as sinusoidal waves when designing IGC laws. However, the disturbances may be affected by various internal and external factors such as actuator imperfections, structural vibrations, environmental factors like wind gusts, and unpredictable interactions with other systems. Therefore, defining the disturbances as pure sinusoidal waves or sum of sinusoids may not be a realistic approach. To provide insight into the effect of observer gain and the presence of randomness in disturbances for the given IGC method, multiple simulations have been performed by determining different disturbances and different ESO gains. Considering the simulation results, random elements in sinusoidal disturbances drastically reduce the IGC law's effectiveness. The observer gains also significantly impact IGC performance, especially for the cases with random elements in disturbances, and determining the appropriate observer gains is considered to have a significant impact on IGC performance.**

I. Introduction

Missile guidance and control is a frequently addressed topic in the defense industry, as the need for precision and efficiency increases with technological advances in military systems. The guidance system of missiles determines the appropriate command to intercept the target, and the control system determines the actuator commands using the guidance command to ensure stability while approaching the target. Most of the conventional missile guidance and control systems are designed separately. This means that the guidance command determined by the guidance system is fed to the control system. In IGC systems, the guidance and control commands are determined and integrated by using the information provided from the target [1]. IGC minimizes the time interval between the guidance command and the actuator deflection. In addition, the control system directly uses target information, which reduces the amount of error that may be present in conventional guidance and control methods. In this study, an IGC scheme based on global terminal SMC [2] is used, and the disturbances caused by system uncertainties, target maneuvers, etc., are estimated by the reduced-order ESO.

In studies [2]-[7], the disturbances are represented with sinusoidal waves or a sum of sinusoids. [3] uses command filtered backstepping to design an IGC system and uses generalized ESO for disturbance estimation. It is stated in [3] that the IGC system has better tracking ability for smooth continuous signals. However, this may not be the case in real-life applications, as stated before. In [4]-[6] observer-based control approaches using SMC are proposed and many numerical simulation results are provided to prove robustness of the systems. In all these studies, stability proof requirements include continuity and boundedness in disturbances and their derivatives. However, determining the disturbances as sinusoids may not be the case in real-life applications, since various internal and external effects might contribute to disturbances, such as actuator imperfections, structural vibrations, environmental factors like wind gusts, and unpredictable interactions with other systems. Therefore, the IGC system is required to achieve the desired performance and stability against disturbances with stochastic characteristics. Since the derivative of the normal distribution is also continuously differentiable and bounded, and the normal distribution itself can be bounded with a high probability [8], it can be used to represent the randomness present in real-life disturbances. This study applies randomness to disturbances by adding normally distributed random numbers to sinusoidal disturbances. Then, the performance of the IGC law against different observer gains is assessed.

II. Mathematical Model

The geometry between the missile and the target is depicted in Figure 1.

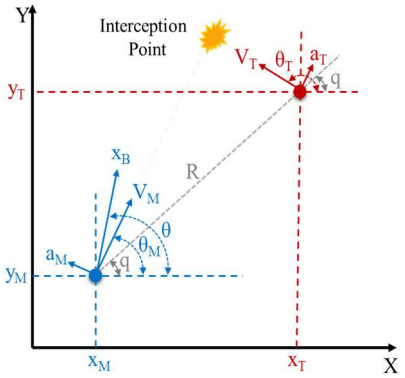

Figure 1 Missile-Target Geometry

The (X_M, Y_M) and (X_T, Y_T) are the missile and target positions on the global X and Y axes, V_M, V_T, a_M, and a_T are

*Research supported by Turkish Aerospace Industries, Inc.

A.B. Author is with the Turkish Aerospace Industries, Inc. and Mechatronics Engineering Department, Cankaya University, Turkey (phone: 090-536-713-3336; e-mail: almila.bektas@tai.com.tr).

H.E. Authot is with the Mechatronics Engineering Department, Çankaya University, Turkey (e-mail: h.ergezer@cankaya.edu.tr).

the missile and target velocity and normal acceleration, x_B is the missile body axis, θ_M and θ_T are the missile and target flight path angles, θ missile pitch angle, q is the line-of-sight (LOS) angle between the missile and the target, and R is the distance between the missile and the target, respectively.

Note that the velocities of the target and the missile are assumed to be constant ($\dot{V}_M = \dot{V}_T = 0$). In Equations (1) to (3), the state space of the IGC model proposed in [2] is given.

$$\begin{cases} \dot{x_1} = x_2 \\ \dot{x_2} = f_2(x_2) + b_2 x_3 + d_2 \\ \dot{x_3} = f_3(x_3) + b_3 x_4 + d_3 \\ \dot{x_4} = f_4(x_4) + b_4 x_5 + d_4 \\ \dot{x_5} = f_5(x_5) + b_5 u \end{cases} \quad (1)$$

where $[x_1, x_2, x_3, x_4, x_5] = [q - q_d, \dot{q} - \dot{q_d}, n_y, \omega_z, \delta_z]$ and q_d is the desired impact angle, n_y is normal overload, ω_z pitch rate, δ_z is the pitch deflection angle, u is control input which corresponds to the pitch deflection angle (δ_{zc}), respectively. The desired impact angle is the angle that the missile is expected to be more effective in terms of destroying the target. The expressions of functions and constants in (2) are given in (3) to (5).

$$\begin{cases} f_2(x_2) = -\frac{2\dot{R}}{R} x_2, & b_2 = -\frac{g\,cos(\theta_M - q)}{R} \\ f_3(x_3) = \left(\frac{g\,sin(\theta_M)}{V_M} - a_1\right) x_3, & b_3 = \frac{a_1 V_M}{g} \\ f_4(x_4) = a_4 x_4 + a_3 \alpha, & b_4 = a_5 \\ f_5(x_5) = -a_6 x_5, & b_5 = a_6 \end{cases} \quad (2)$$

$$\left\{ d_2 = \frac{a_T cos(\theta_T - q)}{R}, \quad d_3 = d_{n_y}, \quad d_4 = d_{\omega_z} \right\} \quad (3)$$

$$\begin{cases} a_1 = \frac{57.3QSc_y^{\alpha}}{mV_M}, & a_2 = \frac{57.3QSc_y^{\delta_z}}{mV_M}, & a_3 = \frac{57.3QSlm_z^{\alpha}}{mV_M}, \\ a_4 = \frac{QSl^2 m_z^{\omega_z}}{J_z V_M}, & a_5 = \frac{57.3QSlm_z^{\delta_z}}{J_z}, & a_6 = \frac{1}{\tau_z}, \end{cases} \quad (4)$$

where, d_{n_y} and d_{ω_z} are system disturbances, m is missile mass, Q is dynamic pressure, S is the aerodynamic reference area, c_y^{α} and $c_y^{\delta_z}$ are derivatives of the lift coefficient, l is the reference length, J_z is the moment of inertia around the Z axis, m_z^{α}, $m_z^{\omega_z}$, $m_z^{\delta_z}$ are aerodynamic moment coefficients, τ_z is time constant, respectively.

The sliding surface equations determined by using global terminal SMC and backstepping control [2] are given in (5) and (6).

$$s_1 = x_2 + \alpha_0 x_1 + \beta_0 x_1^{q_0/p_0} \quad (5)$$

$$\dot{s_1} = -\varphi s_1 - \gamma s_1^{\lambda/\eta} \quad (6)$$

Where α_0 and β_0 are positive constants that determine the SMC starting point, q^0 and p^0 ($\frac{1}{2} < \frac{q_0}{p_0} < 1$) are positive odd integers, $\varphi > 0$ and $\gamma > 0$, determines the speed of reaching the law, λ and η ($\lambda < \eta$) are positive constants, respectively.

The virtual control commands and the control input obtained using the disturbance values estimated by reduced order ESO [2] are given in (7).

$$\begin{cases} x_{3d} = -b_2^{-1}\left[f_2(x_2) + \alpha_0 x_2 + \beta_0 \frac{q_0}{p_0} x_1^{\frac{q_0 - p_0}{p_0}} x_2 + \varphi s_1 + \gamma s_1^{\lambda/\eta} + \widehat{d_2} \right] \\ x_{4d} = b_3^{-1}\left[\dot{x_{3c}} + k_3(x_{3c} - x_3) - f_3(x_3) - \widehat{d_3} \right] \\ x_{5d} = b_4^{-1}\left[\dot{x_{4c}} + k_4(x_{4c} - x_4) - f_4(x_4) - \widehat{d_4} \right] \\ \delta_{zc} = b_5^{-1}[\dot{x_{5c}} + k_5(x_{5c} - x_5) - f_5(x_5)] \end{cases} \quad (7)$$

where k_3, k_4, and k_5 are constants that determine the response speed of the system states. $\widehat{d_2}$, $\widehat{d_3}$, and $\widehat{d_4}$, are the estimated values of d_2, d_3, and d_4 by reduced order ESO.

The reduced order ESO given in [2] is represented by:

$$\begin{cases} \dot{p_2} = -\beta_2 p_2 - \beta_2^2 x_2 - \beta_2[f_2(x_2) + b_2 x_3] \\ \widehat{d_2} = p_2 + \beta_2 x_2 \\ \dot{p_3} = -\beta_3 p_3 - \beta_3^2 x_3 - \beta_3[f_3(x_3) + b_3 x_4] \\ \widehat{d_3} = p_3 + \beta_3 x_3 \\ \dot{p_4} = -\beta_4 p_4 - \beta_4^2 x_4 - \beta_4[f_4(x_4) + b_4 x_5] \\ \widehat{d_4} = p_4 + \beta_4 x_4 \end{cases} \quad (8)$$

where p_2, p_3, and p_4 are auxiliary states and, β_2, β_3, β_4 are observer gains.

III. Simulation Cases

The performance of the IGC model is evaluated in the presence of disturbances. The disturbances for the pure sinusoidal disturbance scenario are given in (3) and in Table 2. Normally distributed random element $N(0, (0.01/\sqrt{2})^2)$ is added to all the disturbances in (3) to represent the randomness in disturbances scenario. The random numbers are generated using *normrnd()* function of MATLAB.

After the performance evaluation in the presence of sinusoidal disturbances with and without random elements, the observer gains given in [2] are increased by 50% and 100%. All the other simulation parameters (also given in [2]) are taken as the same while changing the observer gains. These simulations provide insight into the observer gain effect on estimating the disturbances with random elements by reduced-order ESO. The initial conditions for the simulation are given in Table 1. Any other initial condition that is not shown in the table is zero.

Table 1 Initial Conditions for Simulation

Initial Conditions (at t=0)	
(X_M, Y_M)	(0 m,0 m)
V_M	600 m/s
θ_M	60°
Θ	60°
(X_T, Y_T)	(4330m, 2500m)
θ_T	0°
a_T	50 sin(0.25t) m/s^2
x_1	60°
x_2	-5.15°/s
x_3	0
x_4	0 °/s
x_5	0 °

The simulation input parameters are given in Table 2.

TABLE 2 INPUT PARAMETERS FOR SIMULATION

Simulation Parameters					
a_1	3.1166	$n_{y,\,max.}$	65g	T_3	0.01
a_2	0.2337	$\delta_{zc,\,max.}$	15°	T_4	0.01
a_3	-82.6918	d_{ny}	0.5sin(t)	T_5	0.01
a_4	-0.9749	d_{wz}	0.2sin(t)	ψ	1
a_5	-128.6318	q_0	3	γ	1
a_6	10	p_0	5	λ	1
k_3	10	k_5	8.5	α_0	1
k_4	0.3	η	3	β_0	1

The simulation time is 50 seconds, and the step size is 0.001 seconds. The stop conditions for the simulation are:

- If the missile is getting further from the target,
- If the miss distance is smaller than 10m and the impact angle between the missile and the target is between 20°±1°.

The observer gains β_2, β_3, and β_4 are changed in simulations to observe the performance of IGC for different observer gains. Table 3 shows 15 different simulation cases with 15 sets of observers. The simulations are run for all the cases in Table 3 in the absence and the presence of normally distributed random elements in disturbances. In simulations with random elements, 100 simulations are executed for the same observer gain set. The miss distance and impact angle are assessed by considering the average value of 100 runs.

TABLE 3 OBSERVER GAIN SETS FOR SIMULATION

	CASE	β_2	β_3	β_4
ORIGINAL	1	12	25	20
50% INCREASE	2	18	25	20
	3	12	37.5	20
	4	12	25	30
	5	18	37.5	20
	6	18	25	30
	7	12	37.5	30
	8	18	37.5	30
100% INCREASE	9	24	25	20
	10	12	50	20
	11	12	25	40
	12	24	50	20
	13	24	25	40
	14	12	50	40
	15	24	50	40

IV. SIMULATION RESULTS

Table 4 gives the simulation result of the IGC model with sinusoidal disturbances without random elements. It can be concluded from the table that both impact angle and miss distance objectives are achieved for almost all cases without randomness. However, this scenario is hypothetical since the IGC systems have uncertainties that would not fit a sinusoidal wave in real-life. Case 6 is an exceptional case that cannot satisfy the constraints. The Case 6 simulation history shows it can achieve a 22° impact angle at approximately 300m. However, it then starts to diverge.

TABLE 4 SIMULATION RESULTS OF DISTURBANCE WITHOUT RANDOM ELEMENTS

	Miss Distance (m)	Impact Angle(°)
Case 1	9.8	20.3
Case 2	-205.8	21.0
Case 3	9.8	20.3
Case 4	9.7	20.4
Case 5	-210.0	21.0
Case 6	-0.2	-127.8
Case 7	9.7	20.4
Case 8	0.1	76.3
Case 9	9.7	20.7
Case 10	9.8	20.3
Case 11	9.7	20.4
Case 12	9.8	20.7
Case 13	9.7	20.7
Case 14	9.7	20.4
Case 15	9.8	20.7

The missile and the target trajectories for Case 1 with sinusoidal disturbances only is given in the Figure 2.

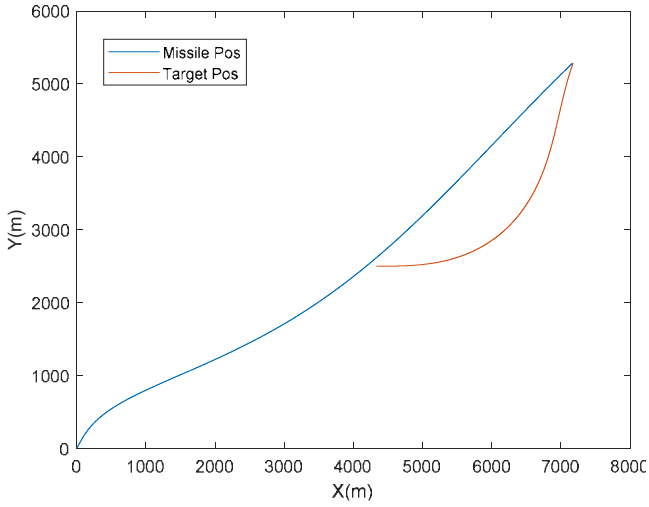

Figure 2 The missile and the target trajectories for Case-1 without randomness in disturbances.

Table 5 gives the percentage of runs that both achieved miss distance and impact angle constraints among 100 runs for each case. It can easily be concluded that the desired miss distance cannot be achieved in average results, and the runs

that give satisfactory results in the presence of randomness are considerably low. According to the analysis results, the miss-distance performance is much poorer than the impact angle performance. This is because the miss distance error is a minimum of 13.5 m, whereas the impact angle error is a minimum of 1.3°. Cases 1, 7, and 14 show the best result regarding the number of results converged in 100 runs. Please note that a 1-2% difference among 100 runs may be misleading, and the overall performance can be better understood if the number of runs for disturbance with random elements is increased.

TABLE 5 SIMULATION RESULTS OF DISTURBANCE WITH RANDOM ELEMENTS (AVERAGE OF 100 RUNS)

	Miss Distance (m)	Impact Angle (°)	% Converged
Case 1	27.0	51.1	4%
Case 2	36.4	21.3	1%
Case 3	24.3	22.4	2%
Case 4	23.5	38.6	3%
Case 5	30.0	37.8	2%
Case 6	54.8	4.9	1%
Case 7	25.4	22.5	4%
Case 8	32.6	49.5	2%
Case 9	659.4	-122.4	2%
Case 10	24.4	28.5	5%
Case 11	26.4	56.9	3%
Case 12	683.0	-131.5	1%
Case 13	670.7	-107.9	0%
Case 14	26.3	39.8	4%
Case 15	664.9	-122.9	2%

The missile and the target trajectories for Case-1 for sinusoidal disturbances with random elements is given in Figure 3.

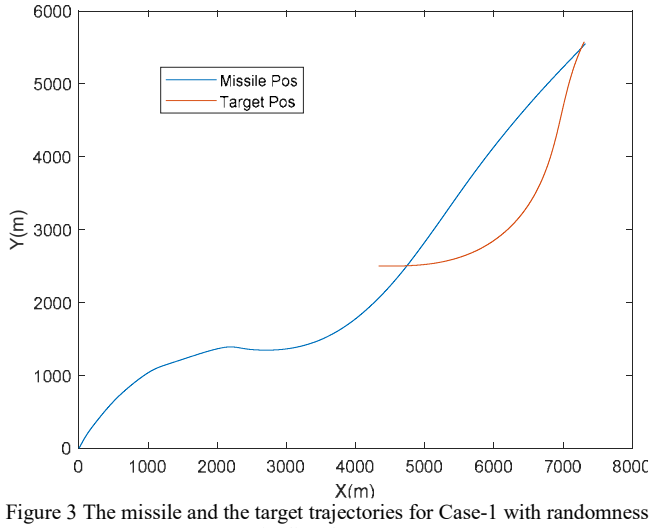

Figure 3 The missile and the target trajectories for Case-1 with randomness in disturbances.

Figure 3 shows that the missile trajectory significantly affected by the presence of random elements in disturbances when compared to the trajectory in Figure 2. The missile flight path length is increased, and impact angle constraint cannot be achieved for the first run.

V. CONCLUSION

The performance of IGC law is assessed in the absence and presence of randomness. In addition, the effect of observer gain on IGC law performance is also evaluated. Simulation results with sinusoidal disturbances show that 11 of 15 cases satisfy the desired impact angle and miss-distance, which corresponds to approximately 73% of all cases. On the other hand, the percentage of the cases that converge in the presence of random elements in disturbances is lower than 5% in any case. As can be concluded from the results, the presence of random elements in sinusoidal disturbances drastically changes the IGC law's effectiveness. The observer gains also significantly impact IGC performance, especially for the cases with random elements in disturbances. Determining the appropriate observer gain for various engagements is worth studying in IGC laws. Future work may focus on developing adaptive or optimization-based methods for online tuning of ESO gains to enhance system performance under varying conditions.

REFERENCES

[1] N. F. Palumbo, B. E. Reardon, and R. A. Blauwkamp "Integrated Guidance and Control for Homing Missiles", *John Hopkins Apl Technical Digest, vol. 25(2), pp. 121-139, 2004.*

[2] Z. Li, Q. Dong, X. Zhang, and Y. Gao, "Impact angle-constrained integrated guidance and control for supersonic skid-to-turn missiles using backstepping with global fast terminal sliding mode control", *Aerospace Science and Technology*, vol. 122, pp 1-17, March 2022.

[3] W. Wang, J. Liu, S. Lin, B. Geng, and Z. Shi, "Command filtered integrated estimation guidance and control for strapdown missiles with circular field of view", *Defence Technology*, vol. 35, pp.211-221, May 2024.

[4] Y. Wang, W. Wang, H. Lei, J. Liu, B. Chen, and Z. Yin, "Observer-based robust impact angle control three-dimensional guidance laws with autopilot lag" *Aerospace Science and Technology*, vol. 141, pp. 1-14, October 2023.

[5] H. Zhang, P. Wang, G. Tang, and W. Bao, "Fuzzy disturbance observer-based dynamic sliding mod control for hypersonic morphing vehicles", *Aerospace Science and Technology*, vol. 142, pp. 1-25, November 2023.

[6] X. Wang, H. Lu, X. Huang, Y. Yang and Z. Zuo, "Three-dimensional time-varying sliding mode guidance law against maneuvering targets with terminal angle constraint", *Chinese Journal of Aeronautics*, vol. 35(4), pp. 303-319, April 2022.

[7] J. Guo, Q. Peng, and Z. Guo, "SMC-Based Integrated Guidance and Control for Beam Riding Missiles with Limited LBPU", vol. 57(5), pp. 2969-2978, October 2021.

[8] M. Harchol-Balter, *Introduction to Probability for Computing*, Cambridge: Cambridge University Press, 2023.